

THREE-DIMENSIONAL INTERFERENCE OF OBLIQUE SHOCK WITH BOUNDARY AND HIGH-ENTROPY LAYERS, AND TECHNIQUES INTENDED FOR INVESTIGATION OF SUCH FLOWS

Volf Ya. Borovoy, Vladimir E. Mosharov, Vladimir N. Radchenko, Anton Yu. Noev

*Central Aerohydrodynamic Institute (TsAGI)
140180 Zhukovsky, Moscow Region, Russia
Email: volf_borovoy@m9com.ru*

Key words: hypersonic flow, interference, boundary layer, high entropy layer, heat transfer, transition, measurement methods

Abstract. Interference between shock waves generated by sharp fins, on the one hand, and boundary layer and high entropy layer generated by blunt leading edge of a plate, on the other hand, has been studied experimentally in short duration wind tunnel UT-1 at Mach numbers $M = 6, 8$ and 10 . The Reynolds number based on the undisturbed flow parameters and plate length was in the range from 5×10^6 at $M = 6$ to 1.5×10^6 at $M = 10$. The boundary layer was laminar ahead the fins, and transition took place inside the separation zone generated by the impinging shock. Three model geometries have been studied: plate without fins, plate with one fin, and plate with two fins generating opposite directed shocks. Heat transfer and pressure distributions have been measured by the help of luminescent temperature sensitive paint (TSP) and pressure sensitive paint (PSP). The study shows that presence of high entropy layer results in significant decrease of heat transfer in the 3D interference regions generated by a single fin or a pair of fins, as well.

1. INTRODUCTION

Interference between an impinging shock wave and a boundary layer is under investigation for more than a half of century^{1,2}. In almost all the papers, the flow over a sharp plate (or a sharp cone) was studied. At the same time, the leading edge of an intake and other elements of a hypersonic vehicle should have certain bluntness. It is required to reduce heating of the leading edge. On the other hand, it is necessary to limit the bluntness radius in order to avoid deteriorations of aerodynamic characteristics of the intake and the entire vehicle.

In the papers^{3,4}, for the first time was systematically studied influence of high-entropy layer generated by a bluntness on heat transfer in the interference region at high Reynolds numbers corresponding to the transitional flow. Two-dimensional impingement of an oblique shock on the flat plate has been investigated. At flow conditions studied (Mach number 6-10, Reynolds number of order 10^6 , laminar-turbulent transitional flow in the interference region), even small bluntness of the plate results in significant weakening of heat exchange in the interference region. The effect increases with Mach number and

bluntness. But existence of threshold bluntness depending on Mach number was revealed: exceeding of the threshold bluntness has small influence on heat transfer in the interference region.

In the present work, similar investigation is extended on three-dimensional flows. The flow formed over the sharp and blunt plates at impingement of inclined shock waves produced by one fin or two fins generating crossing shocks is studied experimentally. The problem is relevant to the overflow of a fin joined with a wing (or fuselage) and of an air intake. It attracted much attention last years (see for example review²). But in the previous papers, overflow only sharp plates has been studied.

Switch to experimental investigation of 3D flows in a short-duration wind tunnel requires development of appropriate measurement methods. This problem is also addressed in this paper.

2. MODELS AND FLOW CONDITIONS

Two similar models have been tested (Figure 1). The first one is intended for heat transfer investigations by the help of temperature sensitive paints (TSP). The main part of the model (the plate **1**) is manufactured from prepreg resin. The length of the plate L is 300 mm, its width $B = 150$ mm. An additional steel plate **4** (its thickness is 3 mm) is fastened to the front surface of the main plate to achieving sharp leading edge. An adapter **5** can be used in order to change bluntness radius of the leading edge in the range from 0 to 4 mm. The second model is intended for measurement of pressure distribution by the help of pressure sensitive paints (PSP). Its main plate **1** was manufactured from aluminum alloy. Therefore the additional plate **4** is not necessary. The same adapters **5** have been used in this case for bluntness variations. On the main plate, one or two fins **2** with different angles can be fastened. Sharp fences **3** have been used for preventing of gas cross flow.

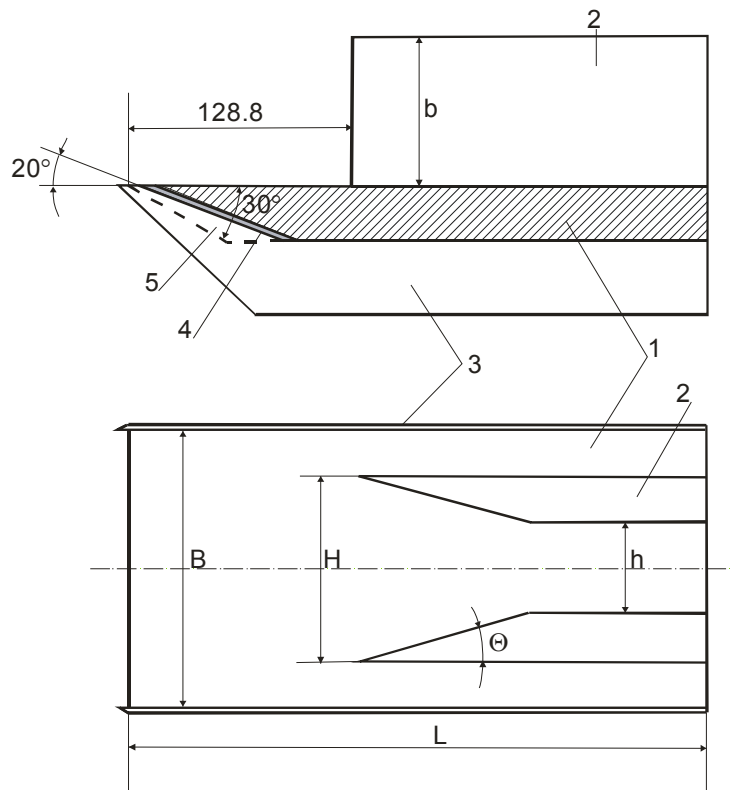


Figure 1. Scheme of the model

The tests have been performed in the short duration facility UT-1 which operates like a Ludwig type wind tunnel. Duration of steady flow is 40 ms. Profiled nozzles were used. The flow parameters are presented in the following table.

M	D,MM	P_t , бар	T_t ,K	$Re_{\infty L} \times 10^{-6}$
6	300	32	725	4.3
8	500	35	740	2.3
10	500	40	760	1.5

Table 1. Flow conditions

3. MEASUREMENT METHODS

3.1. Measurement of heat transfer

Temperature Sensitive Paint application techniques intended for heat flux measurements in Ludwig wind tunnel have been described in 5.6.

3.1.1. Temperature sensitive paint

TSP consists of organic luminophore molecules and polymer binder. It can be made thin enough in order to be used in short duration wind tunnels.

In the present tests, binary (two color) temperature sensitive paint was used. Binary paint contains organic luminophore molecules of two types. One luminophore (europium complex) is temperature sensitive. Its luminescence decreases with temperature growth. Other luminophore (Coumarin) is temperature insensitive. Its luminescence is used as a reference for pixel-by-pixel correction of excitation light variation from flash to flash. Both luminophores are excited simultaneously by UV flash lamp (280-390 nm), but they emit light in two different spectral ranges. Temperature sensitive luminescence is red (580-630 nm), and temperature insensitive luminescence is blue (420-500 nm), thus they can be separated spectrally.

Intensity of emitted red light decreases at temperature increase with the rate of $3 \div 5\%/^{\circ}\text{C}$ and is absolutely insensitive to pressure. TSP is optimized for the temperature range of $10 \div 60^{\circ}\text{C}$. TSP degrades at the temperature above 120°C .

TSP is applied on the model surfaces by spraying like an ordinary paint. The thickness of the dry TSP layer is about $3 \div 5$ micrometers. After TSP application, a set of markers are placed on the model surface. Markers are contrasted (black) points on TSP surface and are used for correction of the model position in the flow and without the flow.

Both images (sensitive and reference) were acquired by one CCD-camera during one exposure using prism image splitter⁷. The prism image splitter contains two identical prisms with different glass filters and is placed in front of camera lens. Naturally, the prism image splitter decreases image size twice. The image splitter was used in present experiment because the window of wind tunnel is too small to install two cameras.

3.1.2. Data processing

Three images are acquired for each wind tunnel run: dark image (without excitation light), wind-off (at known constant temperature) and wind-on images. Each image contains two model images in different spectral ranges and is divided to two separate model images. Thus the number of processed images increases to six.

Data processing includes the next steps:

- Dark signal correction (dark image subtraction);
- Flat field correction;
- Alignment of wind-off and wind-on images using the markers on the model images;

- Pixel-by-pixel correction of excitation light intensity variation: temperature sensitive (red) images are divided on corresponding reference (blue) images;
- Image normalization: wind-on image is divided on corresponding wind-off image. The ratio of 'wind-on' to 'wind-off' images depends only on temperature. It does not depend on paint layer thickness;
- Temperature field calculation using TSP calibration characteristics. TSP calibration is performed in laboratory calibration setup on TSP sample prepared simultaneously with the model covering (*a priori* temperature calibration);
- Heat flux calculation;
- Distortion correction using an image of etalon body;
- Projection of resulting 2D Stanton number field on the 3D mesh describing the model geometry.

3.1.3. Heat flux calculation using temperature measurements

Global heat flux distribution is computed using temperature field by exact solution of one-dimensional heat transfer equation:

$$\begin{aligned} \mathfrak{Q} &= 1 - \exp(-\beta^2) \operatorname{erfc}(\beta) \\ \mathfrak{Q} &= (T_m - T_{in}) / (T_r - T_{in}), \end{aligned} \quad (1)$$

where

T_{in} is the initial model temperature measured by thermocouple before the test start,
 T_m is the model surface temperature measured by TSP at the moment t after the test start,

T_r is the recovery temperature (it is assumed $T_r \approx T_0$),

$\beta = \frac{h\sqrt{t}}{\sqrt{\lambda c \rho}}$ is non-dimensional heat transfer coefficient (h is the heat transfer coefficient),

$\sqrt{\lambda c \rho}$ is heat activity of model material,

erfc is a standard error function.

The results are presented as Stanton number fields ($St = h / \rho_\infty V_\infty C_p$).

3.2 Measurement of pressure

3.2.1. Pressure Sensitive Paint

PSP application in short duration wind tunnel for hypersonic flows was discussed first in⁸. The main requirement to the paint is the fast response to the pressure change.

PSP is a polymeric layer penetrable to oxygen molecules and containing luminophore molecules. Excited by appropriate light source, the luminophore molecules may be transferred to the ground state with light emission (luminescence) or may lose energy by transferring it to oxygen molecules without light emission (luminescence quenching). The part of lost energy is directly proportional to oxygen concentration in the polymer layer and oxygen mobility. Concentration of oxygen in polymer layer is directly proportional to oxygen partial pressure on its external boundary and thus the luminescence output is inversely proportional to oxygen partial pressure (air pressure) above polymer surface.

Response time of PSP is determined by oxygen diffusion in the polymer layer and is directly proportional to the square of layer thickness h and inversely proportional to polymer diffusion coefficient D :

$$\tau = \frac{4h^2}{\pi^2 D} \quad (2)$$

Usage of permeable polymer applied as a very thin layer is a way to decrease response time.

PSP based on silicon resin ($D=1.15 \times 10^{-5}$ cm²/sec) was used in present work (LPS-F2, OPTROD Ltd., Russia). Thus for 99% relaxation of oxygen concentration in PSP layer during wind tunnel run ($3\tau < 40$ ms), the thickness of paint layer should not exceed 5 micrometers. Paint of such thickness is applied easily by air sprayer using diluted solution.

PSP of LPS-F2 type is excited by UV light with wavelength 300÷350 nm and emits blue-green luminescence. Intensity of PSP luminescence decreases about three times at pressure growth from zero to one bar. Temperature sensitivity is about 0.3%/°C at the pressure 1 bar.

3.2.2. Measurement methodology and data processing

Methodology of pressure field measurements is quite similar to temperature field measurements described in Section 3.1, but one-component paint is used for pressure measurements. Data processing includes all the described steps except for the pixel-by-pixel correction of excitation light intensity variation from flash to flash. Only global correction for the whole investigated surface is possible for one-component paint. For this aim, a spot of Luminescent Reference Paint (LRP) is applied on the model surface. LRP is a luminescent material which is insensitive both to temperature and pressure. Luminescent signal of LRP is used for excitation light correction: each image is divided on average LRP intensity.

Wind-off images were acquired before wind tunnel start at zero pressure. Wind-on images were acquired at the end of wind tunnel run (with 40 ms delay after flow initialization). Some runs were fulfilled with 20 ms delay in order to be confident that PSP response time is small enough.

Model for PSP measurements was made from aluminum to decrease temperature influence on measurement results. It was assumed that PSP temperature does not change during the run and is equal to the model temperature before the test. Pressure field was calculated using *a priori* PSP calibration. PSP calibration was performed in laboratory calibration setup on PSP sample prepared simultaneously with the model covering.

4. HEAT TRANSFER

4.1. Plate without fins

The experimental results testify to the laminar state of the boundary layer over the most part of the plate: the data coincide with calculations of laminar boundary layer (Figure 2) (some discrepancy near the leading edge is probably caused by the junction between the additional steel plate **4** and the main plate **1**, Figure 1). Here and below the Stanton number presents itself the ratio of measured heat flux to the difference between the total temperature and the surface temperature.

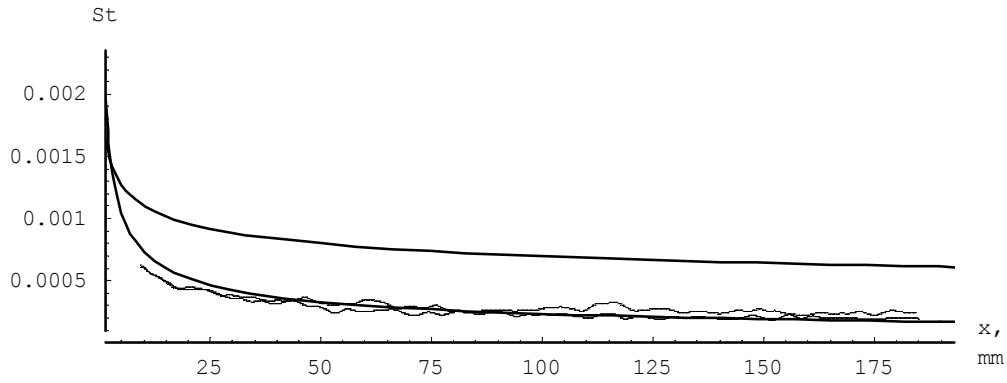


Figure 2. Distribution of Stanton number along the plate (M=6)

At Mach number 6, laminar-turbulent transition takes place only in narrow longitudinal strips. They are provoked by micro irregularities of the leading edge. In the strips, the transition starts at the distance 150-200mm from the leading edge and does not finish to the end of the plate.

Similar results have been obtained at Mach numbers 8 and 10, but increase of Mach number and corresponding decrease of absolute values of heat flux results in augmentation of random error of data.

4.2. Plate with one fin

Figure 3 presents fields of Stanton number values on the plate near a single fin which have been obtained at two experiments. They differ only in bluntness of the plate. A narrow strip of high heat transfer is created between the shock and the fin (nearer to the fin). There is also visible that bluntness leads to significant weakening of heat transfer in the interference region: at presence of bluntness, the region of high heat transfer become smaller and the maximum heat transfer coefficient decreases.

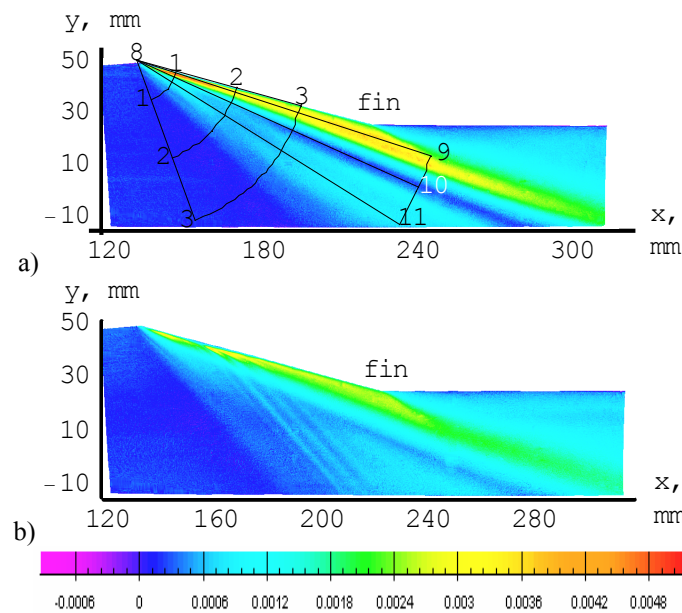


Figure 3. Stanton number distribution near the fin with angle $\theta = 15^\circ$ at Mach number $M = 6$: a) on the sharp plate, b) on the blunt one with bluntness radius $r = 0.5$ mm

In the range of bluntness radii from 0.1 to 0.5 mm, a periodical system of strips forms in the forward part of the interference region (see Figure 3b). Maximum values of Stanton number in the strips exceed the minimal ones located between the strips on 25-60%. Distance between the strips (wave length) in direction of undisturbed flow is 5-6 mm which is several times bigger than the thickness of boundary layer ($\delta \sim 1$ mm). Inclination angle of the strips is approximately 50° relative the undisturbed flow. Presence of the strip system can be connected with instability of the laminar boundary layer in the interference region in front of shock wave.

For graphical presentation of data, the polar coordinate system shown on the Figure 3a is used. Its origin coincides with the fin leading edge and the angle φ of the rays is counted clock wise from the fin surface. From theoretical point of view, the viscid-gas flow near the fin can not be considered as a conical one. But analysis of many tests performed show that variation of heat transfer coefficient along a ray is small at related distances from the fin leading edge $R/X_o \geq 0.3$ for Mach number $M=6$ and at $R/X_o \geq 0.5$ for $M=8$ ($X_o=130.5$ mm is the distance from the plate leading edge to the fin leading edge). This is why the polar coordinate system is used in this investigation.

Figure 4 presents distributions of relative Stanton numbers on the sharp plate obtained in two repetitive experiments. The distributions correspond to the arc cross section 3 (see Figure 3a) with relative radius $R/X_o = 0.5$. The experimental values of Stanton number St are related to St_o which is the calculated value for the point X_o . Results of two repeated tests practically coincide. Good repetition was confirmed in many tests at Mach number 6. At higher Mach numbers, the repetition is not so good.

The vertical line on Figure 4 depicts shock location in the inviscid gas. The influence region of the fin is restricted by the ray $\varphi \approx 35^\circ$. For $\varphi > 35^\circ$, the ratio St/St_o is close to 1. The maximum of Stanton number is located on the ray $\varphi = 3^\circ - 4^\circ$, i.e. between the fin surface ($\varphi = 0$) and the shock wave ($\varphi = 7.65^\circ$). At considerable distance from the fin leading edge ($R/X_o \geq 0.3$), a plato forms with approximately constant values of Stanton numbers. It is located in the range $\varphi = 10^\circ - 20^\circ$.

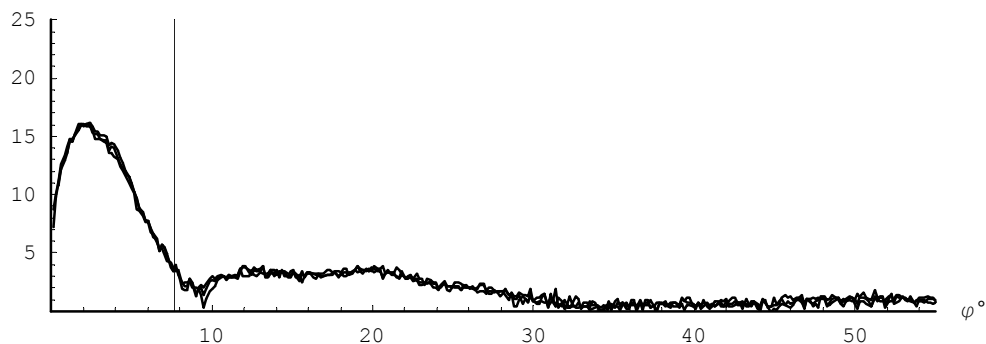


Figure 4. Distribution of related Stanton number values over the sharp plate ($r = 0$) at $M=6$ in the cross section 3 (see Figure 3a); radius of the arc is $R = 66$ mm ($R/X_o = 0.5$)

Figure 5 demonstrates influence of plate bluntness on cross distribution of heat transfer coefficient. Plate bluntness decreases heat transfer significantly and diminishes unevenness of heat transfer distribution in the interference region.

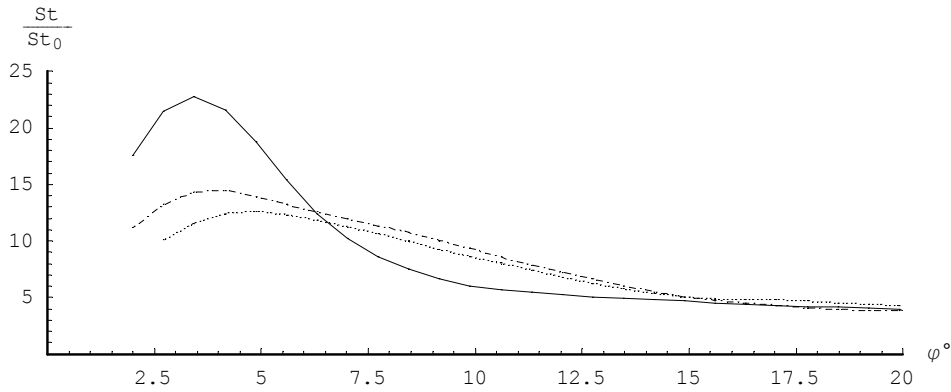


Figure 5. Influence of plate bluntness on heat transfer distribution in the cross section 3, $R/X_o = 0.3$ (see Figure 3): solid line $r=0$, dotted line $r = 0.5$ mm, chain line $r = 1.0$ mm

Influence of plate bluntness on the maximal value of related Stanton number in three cross sections is shown in the Figure 6. Here St_{mb} is maximal value on the blunt plate, St_{mo} is similar one on the sharp plate, and δ^* is displacement thickness of the laminar boundary layer in the point X_o . Bluntness results in significant decrease (approximately 1.5 times) of the maximal Stanton number at considerable distance from the fin leading edge. At small distance from the fin leading edge (in the section 1), non monotonic variation of the ratio St_{mb}/St_{mo} is visible. It is connected with movement in forward direction of the hot strip (existing behind the shock wave) caused by the bluntness of the plate.

At increase of bluntness, stabilisation of hear exchange occurs beginning from some bluntness dimension. It means that further increase of bluntness does not significant effect on the maximal value of heat transfer coefficient. Near the fin leading edge (at $R/X_o = 0.12$), stabilisation comes at $r/\delta^* \approx 0.2$, and far from the fin leading edge it happens at $r/\delta^* \approx 1$. Similar phenomenon has been observed at 2D interference flow⁹. The present work differs from⁹ not only due to 3D flow but also due bigger distance between the plate leading edge and the shock. Similar results have been obtained at higher Mach numbers $M=8$ and 10 .

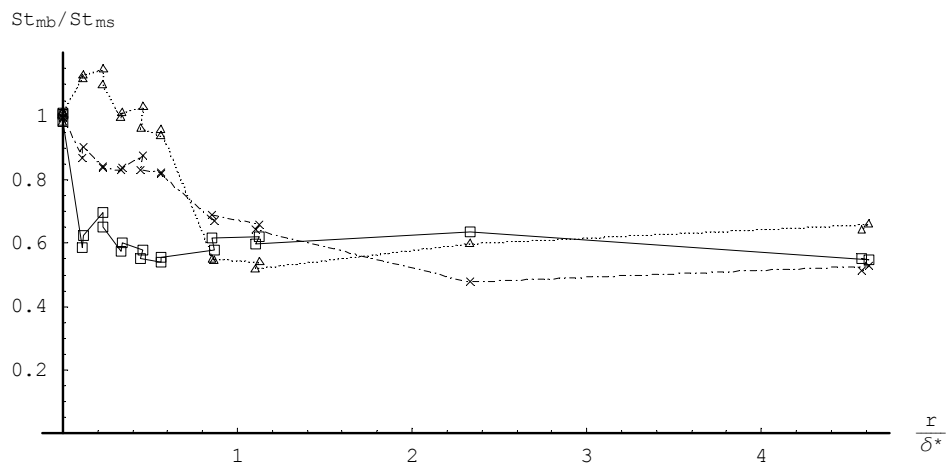


Figure 6. Bluntness influence on maximal Stanton number in three cross sections (see Figure 3) at $M=6$: solid line - section 1, dashed line - section 2, chain line - section 3.

4.3. Plate with two fins

Figure 7 presents distribution of Stanton number near two similar fins generating opposite directed shock waves. Near the leading edges where the fins do not interfere with each other, a narrow strip of high heat transfer is created near both fins (between the shock and fin surface). Ahead the strips, wider zones of slightly intensified heat transfer are situated. The intensification is caused by separation shocks and pressure increase in front of them. Interference between the fins leads to an additional augmentation of heat transfer both at intersection of the main shocks (generated by the fins) and at intersection of the secondary shocks (generated by the separation zones), as well (Figure 7a). Bluntness of the plate results in significant decrease of heat transfer in both zones (Figure 7b). Unfortunately, the heat transfer distribution between the fins is non symmetric. On the one hand, this is due to error in mounting of the fins, and on the other hand, due to high sensitivity of heat transfer in the interference region to the flow direction.

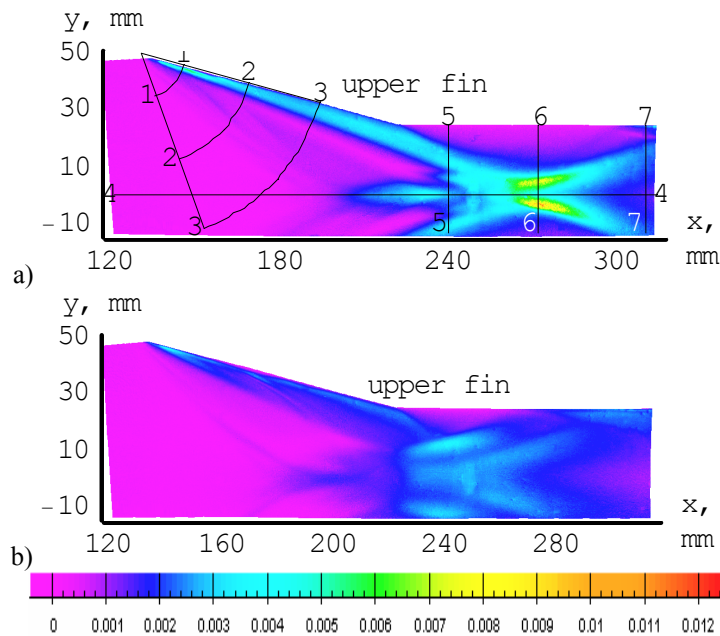


Figure 7. Stanton number distribution near two fins with angle $\theta = 15^\circ$ at Mach number $M = 6$: a) on the sharp plate, b) on the blunt one with bluntness radius $r = 1.0$ mm

For quantitative analysis, 7 sections shown on Figure 7a have been chosen. The data obtained for the three first sections confirm that distributions of Stanton numbers near a single fin and a pair of fins practically coincide in this region both on the sharp plate and on the blunt one (for example on Figure 8, comparison is performed for the section 1). It means that in the case of pair fins, they are streamlined by a supersonic flow, i.e. the “supersonic start” of the channel formed between the fins takes place. According the calculation, for supersonic start at Mach number 6, the related width of the channel should be $h/H \geq 0.634$. In reality, the related width of the model tested (see Figure 1) was smaller: $h/H = 0.5$, but the start takes place. It happened probably because the channel was not closed fully. In addition, “the wave start” of the flow in the impulse type wind tunnel UT-1 can also promote start of supersonic flow inside a narrowed channel. Coincidence of the data for the single fin and the pair fins near the leading edges testifies again to good repetition of the test results at $M=6$. At last, Figure 8 demonstrates significant diminishing of heat transfer in the forward part of interference region due to the plate bluntness.

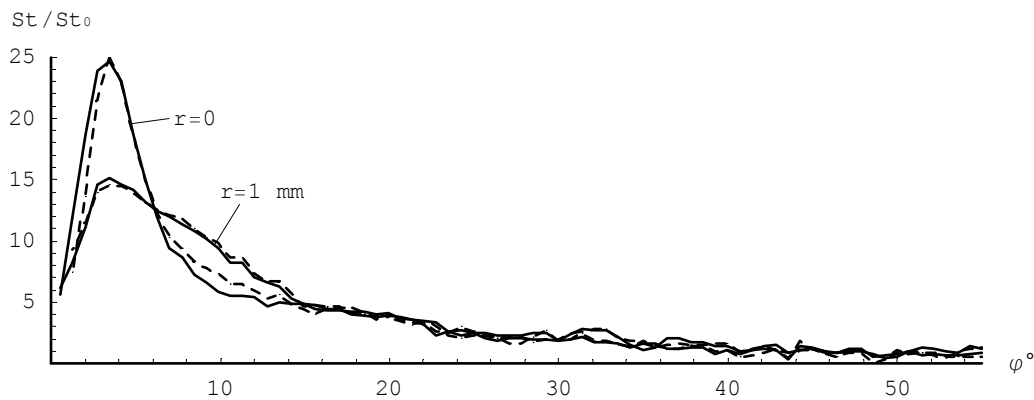


Figure 8. Distribution of Stanton number in the cross section 1 ($R/X_o = 0.12$, see Figure 7a) over the sharp ($r = 0$) and blunt ($r = 1$ mm) plates: solid lines – single fin, dashed lines – pair fins.

The distribution of Stanton number along the channel axis is depicted on the Figure 9. It is interesting particularly due to information concerning heat transfer in region of intersection of separation zones and secondary shock waves generated by the separation zones (see Figure 7a, $X=180-240$ mm). At intersection of the secondary shock waves, the ratio St/St_o achieves on the sharp plate the value 15-20 (Figure 9, $r = 0$, $X = 230$ mm), where as near the single fin (Figure 4, $\varphi = 12^\circ-20^\circ$) and near the fin leading edges of pair fins (Figure 8) $St/St_o \approx 4$. Blunting of the plate results in diminishing of the ratio from the value 15-20 to about 10 (see Figure 9, $r = 1$ mm).

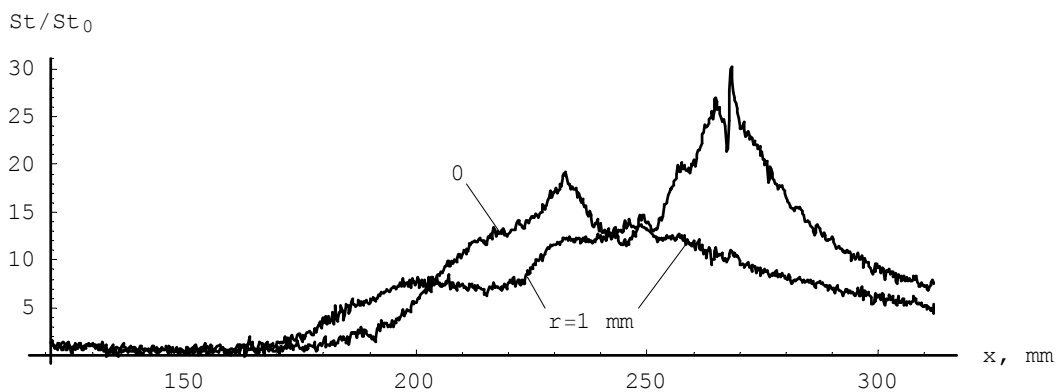


Figure 9. Distribution of Stanton number along the symmetry line between two fins (section 4, see Figure 7a).

The heat transfer coefficient achieves its maximal value in two strips near the shocks reflected from the symmetry line (yellow spots on Figure 7a). Here the ratio St/St_o on the sharp plate is about 40-60 (Figure 10a, section 6). These zones would be very difficult to reveal by the help of sensors. Blunting of the plate with radius 1mm decreases the maximal Stanton number more than 3 times (Figure 10b, section 6).

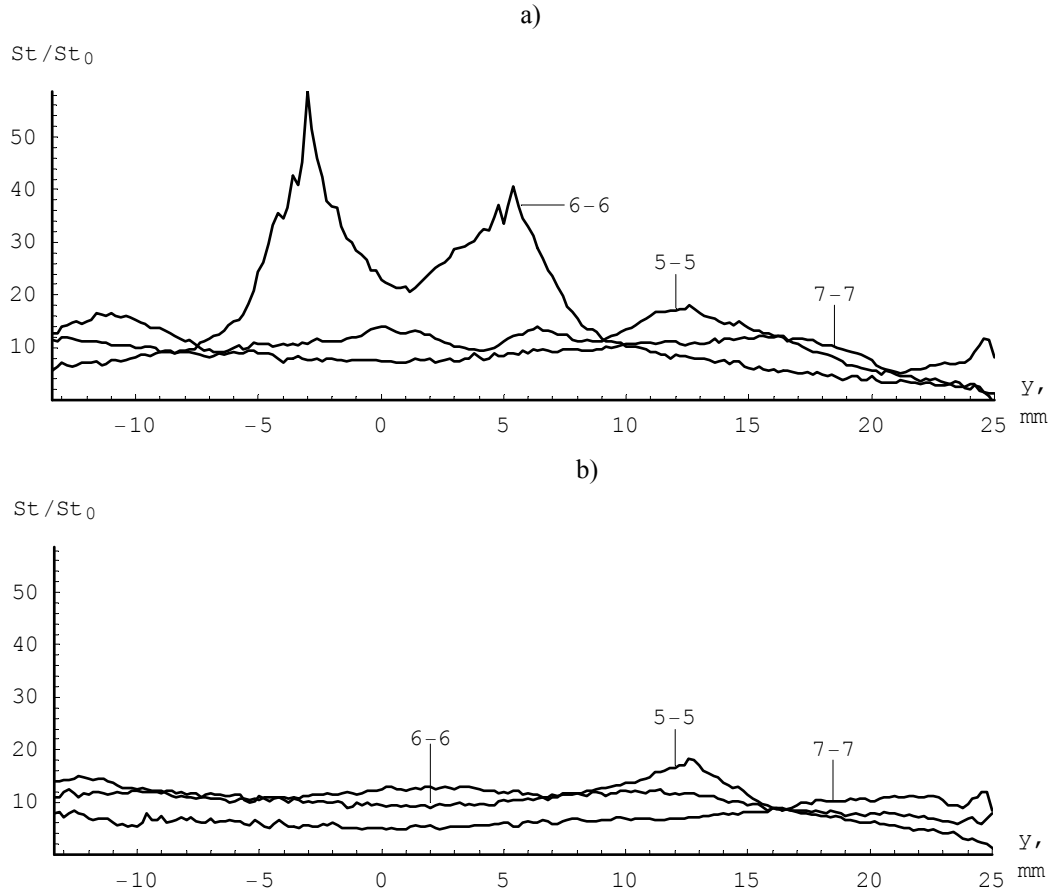


Figure 10. Distribution of Stanton number on the plates with two fins in three cross sections (see Figure 7a): a) on the sharp plate ($r=0$), b) on the blunt one ($r=1$ mm).

5. PRESSURE DISTRIBUTION

Systematic investigation of pressure distribution was not performed. Only preliminary tests have been fulfilled. The main aim of this section is to demonstrate possibilities of the PSP method in short duration wind tunnel.

Pressure fields were measured at Mach number 6 on the plate with leading edge blunting radius 0.1 mm. One fin and two fin model configurations were tested. Only fins with wedge angle 20 deg have been tested. Pressure on the fin surface itself was measured in several runs. Roll angle of the model was adjusted to illuminate only one investigated surface: plate surface or fin surface (both surfaces were covered by PSP). Such technique helped to exclude reflection of luminescence light from one surface onto another one (reillumination).

Figure 11 depicts pressure distribution over the surface of a single fin mounted on a sharp plate. It demonstrates high sensitivity of the luminescent paint: one can see a region of small pressure increase being a trace of weak wave generated by the boundary layer of the plate.

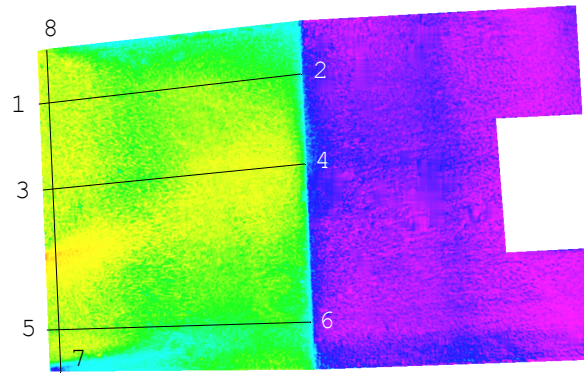


Figure 11. Pressure field on the fin with angle $\theta=20^\circ$ at Mach number $M = 6$

On the Figure 12, pressure distribution on the fin along the flow direction is shown. The horizontal dashed line corresponds to the pressure over the fin behind the oblique shock in inviscid gas $P = 12500$ Pa (the calculated pressure in the undisturbed flow is 1350 Pa). It is evident that the data agree with the prediction.

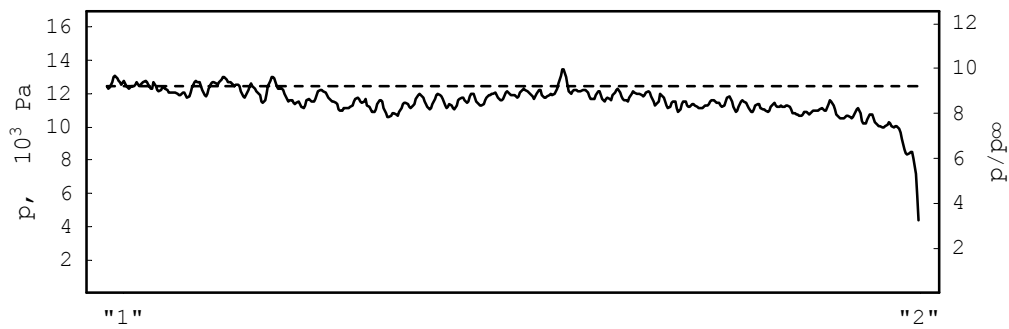


Figure 12. Pressure distribution on the fin in the section 1-2 (see Figure 11)

Figure 13 presents pressure distribution on the sharp plate with a single fin. One can see the narrow strip of high pressure between the shock and fin surface. In addition, there is visible weak pressure increase due to boundary layer separation and presence of secondary shock in front of the main oblique shock generated by the fin.

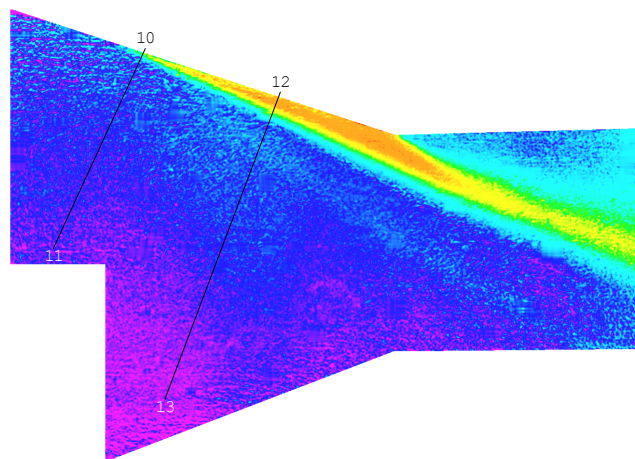


Figure 13. Pressure field on the sharp plate near a single fin with angle $\theta = 20^\circ$ at $M = 6$

On Figure 14 is shown the pressure field on the sharp plate with a pair of fins. One can see regions of pressure increase at intersection of shock waves. The Figure depicts non symmetry of the flow due error in mounting of the fins: inclination angle of the lower fin is bigger than of the upper one.

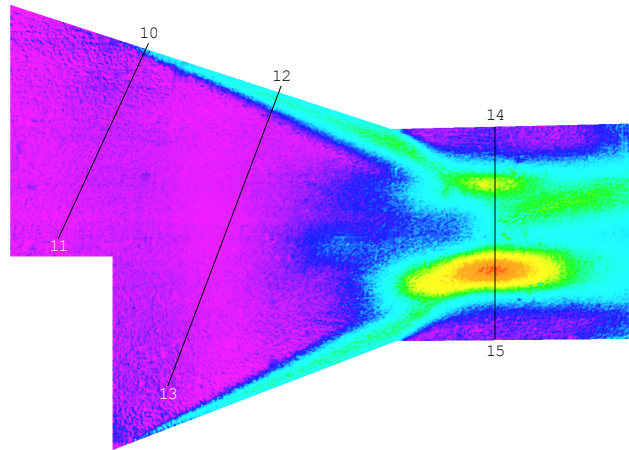


Figure 14. Pressure field on the sharp plate near a pair of fins with angle $\theta=20^\circ$ at $M = 6$

6. CONCLUSION

Heat transfer and pressure distribution over a plate near a single fin and a pair of fins have been studied experimentally at laminar state of the undisturbed boundary layer.

The data show that at hypersonic speed, plate bluntness results in significant weakening of heat exchange in the three-dimensional interference flows. This phenomenon is similar to one observed at two-dimensional interference of shock wave with boundary and high entropy layers. Especially big impact of plate bluntness was obtained in the channel created between two fins generating opposite directed shocks.

The experience confirms that luminescent Temperature Sensitive Paints and Pressure Sensitive Paints are very useful at investigations of 3D flows in short duration wind tunnels.

The work was performed under support of Russian Foundation for Basic Researches (Project No. 05-01-00557a).

7. REFERENCES

- [1] D.S. Dolling Fifty Years of Shock-Wave / Boundary-Layer Interaction Research: What Next? *AIAA Journal*, V. 39. No. 8. P. 1517- 1531 (2001).
- [2] A.A. Zheltovodov Advances and Problems in Modeling of Shock Wave Turbulent Boundary layer interactions. *XII Intern. Conf. on the Methods of Aerophysical Research*, Novosibirsk., pp. 225-236 (2004).
- [3] V.Ya. Borovoi, I.V. Egorov, A.S. Skuratov, and I.V. Struminskaya, Effect of a high-entropy layer on heat transfer in the region of the incidence of an oblique shock wave on a blunted-plate surface. *Doklady Physics*. Vol.50, No.1, pages 3-6 (2005).

- [4] V.Ya. Borovoi, I.V. Egorov, A.S. Skuratov, and I.V. Struminskaya, Interaction between an inclined shock and boundary and high-entropy layer on a flat plate. *Fluid Dynamics*. Vol.40. No.6, pages 911-928 (2005).
- [5] V.E. Mosharov, A.A. Orlov, V.N. Radchenko "Temperature Sensitive Paint (TSP) for Heat Transfer Measurement in Short Duration Wind Tunnels" *20th ICIASF Congress*, Goettingen, Germany, August 25-29, 2003.
- [6] V.E. Mosharov, V.N. Radchenko, "Heat transfer measurements in short-duration wind tunnel by Temperature Sensitive Paint," *TsAGI, Uchenye Zapiski*, vol.38, No1-2, 2007 (in Russian).
- [7] V.P. Kulesh, A.N. Morozov, V.E. Mosharov and V.N. Radchenko "The application of prism image splitter for pressure distribution measurement using the method of two-color luminescent sensors", *Instruments and Experimental Techniques*, vol.44, No1, (2001).
- [8] V.Ya. Borovoi, A.P. Bykov, V.E. Mosharov, A.A. Orlov, V.N. Radchenko, S.D. Phonov "Pressure Sensitive Paint Application in Shock Wind Tunnel" *ICIASF 95*, 4p., July10 – 11, 1995
- [9] V.Ya. Borovoi, A.S. Skuratov, and I.V. Struminskaya, About presence of "threshold" bluntness of a plate at interference between an oblique shock and boundary and entropy layers. To be published in *Fluid Dynamics*, (2008)